

Search for Long-Lived Doubly Charged Higgs Bosons in $p\bar{p}$ Collisions at $\sqrt{s} = 1.96$ TeV

- D. Acosta,¹⁶ J. Adelman,¹² T. Affolder,⁹ T. Akimoto,⁵⁴ M. G. Albrow,¹⁵ D. Ambrose,¹⁵ S. Amerio,⁴² D. Amidei,³³
 A. Anastassov,⁵⁰ K. Anikeev,¹⁵ A. Annovi,⁴⁴ J. Antos,¹ M. Aoki,⁵⁴ G. Apollinari,¹⁵ T. Arisawa,⁵⁶ J.-F. Arguin,³²
 A. Artikov,¹³ W. Ashmanskas,¹⁵ A. Attal,⁷ F. Azfar,⁴¹ P. Azzi-Bacchetta,⁴² N. Bacchetta,⁴² H. Bachacou,²⁸ W. Badgett,¹⁵
 A. Barbaro-Galtieri,²⁸ G. J. Barker,²⁵ V. E. Barnes,⁴⁶ B. A. Barnett,²⁴ S. Baroiant,⁶ G. Bauer,³¹ F. Bedeschi,⁴⁴ S. Behari,²⁴
 S. Belforte,⁵³ G. Bellettini,⁴⁴ J. Bellinger,⁵⁸ A. Belloni,³¹ E. Ben-Haim,¹⁵ D. Benjamin,¹⁴ A. Beretvas,¹⁵ A. Bhatti,⁴⁸
 M. Binkley,¹⁵ D. Bisello,⁴² M. Bishai,¹⁵ R. E. Blair,² C. Blocker,⁵ K. Bloom,³³ B. Blumenfeld,²⁴ A. Bocci,⁴⁸ A. Bodek,⁴⁷
 G. Bolla,⁴⁶ A. Bolshov,³¹ D. Bortoletto,⁴⁶ J. Boudreau,⁴⁵ S. Bourou,¹⁵ B. Brau,⁹ C. Bromberg,³⁴ E. Brubaker,¹²
 J. Budagov,¹³ H. S. Budd,⁴⁷ K. Burkett,¹⁵ G. Busetto,⁴² P. Bussey,¹⁹ K. L. Byrum,² S. Cabrera,¹⁴ M. Campanelli,¹⁸
 M. Campbell,³³ F. Canelli,⁷ A. Canepa,⁴⁶ M. Casarsa,⁵³ D. Carlsmith,⁵⁸ R. Carosi,⁴⁴ S. Carron,¹⁴ M. Cavalli-Sforza,³
 A. Castro,⁴ P. Catastini,⁴⁴ D. Cauz,⁵³ A. Cerri,²⁸ L. Cerrito,⁴¹ J. Chapman,³³ Y. C. Chen,¹ M. Chertok,⁶ G. Chiarelli,⁴⁴
 G. Chlachidze,¹³ F. Chlebana,¹⁵ I. Cho,²⁷ K. Cho,²⁷ D. Chokheli,¹³ J. P. Chou,²⁰ S. Chuang,⁵⁸ K. Chung,¹¹ W.-H. Chung,⁵⁸
 Y. S. Chung,⁴⁷ M. Cijliak,⁴⁴ C. I. Ciobanu,²³ M. A. Ciocci,⁴⁴ A. G. Clark,¹⁸ D. Clark,⁵ M. Coca,¹⁴ A. Connolly,²⁸
 M. Convery,⁴⁸ J. Conway,⁶ B. Cooper,³⁰ K. Copic,³³ M. Cordelli,¹⁷ G. Cortiana,⁴² J. Cranshaw,⁵² J. Cuevas,¹⁰ A. Cruz,¹⁶
 R. Culbertson,¹⁵ C. Currat,²⁸ D. Cyr,⁵⁸ D. Dagenhart,⁵ S. Da Ronco,⁴² S. D'Auria,¹⁹ P. de Barbaro,⁴⁷ S. De Cecco,⁴⁹
 A. Deisher,²⁸ G. De Lentdecker,⁴⁷ M. Dell'Orso,⁴⁴ S. Demers,⁴⁷ L. Demortier,⁴⁸ M. Deninno,⁴ D. De Pedis,⁴⁹
 P. F. Derwent,¹⁵ C. Dionisi,⁴⁹ J. R. Dittmann,¹⁵ P. DiTuro,⁵⁰ C. Dörr,²⁵ A. Dominguez,²⁸ S. Donati,⁴⁴ M. Donega,¹⁸
 J. Donini,⁴² M. D'Onofrio,¹⁸ T. Dorigo,⁴² K. Ebina,⁵⁶ J. Efron,³⁸ J. Ehlers,¹⁸ R. Erbacher,⁶ M. Erdmann,²⁵ D. Errede,²³
 S. Errede,²³ R. Eusebi,⁴⁷ H.-C. Fang,²⁸ S. Farrington,²⁹ I. Fedorko,⁴⁴ W. T. Fedorko,¹² R. G. Feild,⁵⁹ M. Feindt,²⁵
 J. P. Fernandez,⁴⁶ R. D. Field,¹⁶ G. Flanagan,³⁴ L. R. Flores-Castillo,⁴⁵ A. Foland,²⁰ S. Forrester,⁶ G. W. Foster,¹⁵
 M. Franklin,²⁰ J. C. Freeman,²⁸ Y. Fujii,²⁶ I. Furic,¹² A. Gajjar,²⁹ M. Gallinaro,⁴⁸ J. Galyardt,¹¹ M. Garcia-Sciveres,²⁸
 A. F. Garfinkel,⁴⁶ C. Gay,⁵⁹ H. Gerberich,¹⁴ D. W. Gerdes,³³ E. Gerchtein,¹¹ S. Giagu,⁴⁹ P. Giannetti,⁴⁴ A. Gibson,²⁸
 K. Gibson,¹¹ C. Ginsburg,¹⁵ K. Giolo,⁴⁶ M. Giordani,⁵³ M. Giunta,⁴⁴ G. Giurgiu,¹¹ V. Glagolev,¹³ D. Glenzinski,¹⁵
 M. Gold,³⁶ N. Goldschmidt,³³ D. Goldstein,⁷ J. Goldstein,⁴¹ G. Gomez,¹⁰ G. Gomez-Ceballos,¹⁰ M. Goncharov,⁵¹
 O. González,⁴⁶ I. Gorelov,³⁶ A. T. Goshaw,¹⁴ Y. Gotra,⁴⁵ K. Goulianatos,⁴⁸ A. Gresele,⁴² M. Griffiths,²⁹ C. Grossi-Pilcher,¹²
 U. Grundler,²³ J. Guimaraes da Costa,²⁰ C. Haber,²⁸ K. Hahn,⁴³ S. R. Hahn,¹⁵ E. Halkiadakis,⁴⁷ A. Hamilton,³²
 B.-Y. Han,⁴⁷ R. Handler,⁵⁸ F. Happacher,¹⁷ K. Hara,⁵⁴ M. Hare,⁵⁵ R. F. Harr,⁵⁷ R. M. Harris,¹⁵ F. Hartmann,²⁵
 K. Hatakeyama,⁴⁸ J. Hauser,⁷ C. Hays,¹⁴ H. Hayward,²⁹ B. Heinemann,²⁹ J. Heinrich,⁴³ M. Hennecke,²⁵ M. Herndon,²⁴
 C. Hill,⁹ D. Hirschbuehl,²⁵ A. Hocker,¹⁵ K. D. Hoffman,¹² A. Holloway,²⁰ S. Hou,¹ M. A. Houlden,²⁹ B. T. Huffman,⁴¹
 Y. Huang,¹⁴ R. E. Hughes,³⁸ J. Huston,³⁴ K. Ikado,⁵⁶ J. Incandela,⁹ G. Introzzi,⁴⁴ M. Iori,⁴⁹ Y. Ishizawa,⁵⁴ C. Issever,⁹
 A. Ivanov,⁶ Y. Iwata,²² B. Iyutin,³¹ E. James,¹⁵ D. Jang,⁵⁰ B. Jayatilaka,³³ D. Jeans,⁴⁹ H. Jensen,¹⁵ E. J. Jeon,²⁷ M. Jones,⁴⁶
 K. K. Joo,²⁷ S. Y. Jun,¹¹ T. Junk,²³ T. Kamon,⁵¹ J. Kang,³³ M. Karagoz Unel,³⁷ P. E. Karchin,⁵⁷ Y. Kato,⁴⁰ Y. Kemp,²⁵
 R. Kephart,¹⁵ U. Kerzel,²⁵ V. Khotilovich,⁵¹ B. Kilminster,³⁸ D. H. Kim,²⁷ H. S. Kim,²³ J. E. Kim,²⁷ M. J. Kim,¹¹
 M. S. Kim,²⁷ S. B. Kim,²⁷ S. H. Kim,⁵⁴ Y. K. Kim,¹² M. Kirby,¹⁴ L. Kirsch,⁵ S. Klimenko,¹⁶ M. Klute,³¹ B. Knuteson,³¹
 B. R. Ko,¹⁴ H. Kobayashi,⁵⁴ D. J. Kong,²⁷ K. Kondo,⁵⁶ J. Konigsberg,¹⁶ K. Kordas,³² A. Korn,³¹ A. Korytov,¹⁶
 A. V. Kotwal,¹⁴ A. Kovalev,⁴³ J. Kraus,²³ I. Kravchenko,³¹ A. Kreymer,¹⁵ J. Kroll,⁴³ M. Kruse,¹⁴ V. Krutelyov,⁵¹
 S. E. Kuhlmann,² S. Kwang,¹² A. T. Laasanen,⁴⁶ S. Lai,³² S. Lami,^{44,48} S. Lammel,¹⁵ M. Lancaster,³⁰ R. Lander,⁶
 K. Lannon,³⁸ A. Lath,⁵⁰ G. Latino,⁴⁴ R. Lauhakangas,²¹ I. Lazzizzera,⁴² C. Lecci,²⁵ T. LeCompte,² J. Lee,²⁷ J. Lee,⁴⁷
 S. W. Lee,⁵¹ R. Lefèvre,³ N. Leonardo,³¹ S. Leone,⁴⁴ S. Levy,¹² J. D. Lewis,¹⁵ K. Li,⁵⁹ C. Lin,⁵⁹ C. S. Lin,¹⁵ M. Lindgren,¹⁵
 E. Lipeles,⁸ T. M. Liss,²³ A. Lister,¹⁸ D. O. Litvintsev,¹⁵ T. Liu,¹⁵ Y. Liu,¹⁸ N. S. Lockyer,⁴³ A. Loginov,³⁵ M. Loreti,⁴²
 P. Loverre,⁴⁹ R.-S. Lu,¹ D. Lucchesi,⁴² P. Lujan,²⁸ P. Lukens,¹⁵ G. Lungu,¹⁶ L. Lyons,⁴¹ J. Lys,²⁸ R. Lysak,¹ E. Lytken,⁴⁶
 D. MacQueen,³² R. Madrak,¹⁵ K. Maeshima,¹⁵ P. Maksimovic,²⁴ G. Manca,²⁹ R. Marginean,¹⁵ C. Marino,²³ A. Martin,⁵⁹
 M. Martin,²⁴ V. Martin,³⁷ M. Martínez,³ T. Maruyama,⁵⁴ H. Matsunaga,⁵⁴ M. Mattson,⁵⁷ P. Mazzanti,⁴ K. S. McFarland,⁴⁷
 D. McGivern,³⁰ P. M. McIntyre,⁵¹ P. McNamara,⁵⁰ R. McNulty,²⁹ A. Mehta,²⁹ S. Menzemer,³¹ A. Menzione,⁴⁴ P. Merkel,⁴⁶
 C. Mesropian,⁴⁸ A. Messina,⁴⁹ T. Miao,¹⁵ N. Miladinovic,⁵ J. Miles,³¹ L. Miller,²⁰ R. Miller,³⁴ J. S. Miller,³³ C. Mills,⁹
 R. Miquel,²⁸ S. Miscetti,¹⁷ G. Mitselmakher,¹⁶ A. Miyamoto,²⁶ N. Moggi,⁴ B. Mohr,⁷ R. Moore,¹⁵ M. Morello,⁴⁴
 P. A. Movilla Fernandez,²⁸ J. Muelmenstaedt,²⁸ A. Mukherjee,¹⁵ M. Mulhearn,³¹ T. Muller,²⁵ R. Mumford,²⁴ A. Munar,⁴³
 P. Murat,¹⁵ J. Nachtman,¹⁵ S. Nahm,⁵⁹ I. Nakano,³⁹ A. Napier,⁵⁵ R. Nabora,²⁴ D. Naumov,³⁶ V. Necula,¹⁶ J. Nielsen,²⁸
 T. Nelson,¹⁵ C. Neu,⁴³ M. S. Neubauer,⁸ T. Nigmanov,⁴⁵ L. Nodulman,² O. Norniella,³ T. Ogawa,⁵⁶ S. H. Oh,¹⁴ Y. D. Oh,²⁷

T. Ohsugi,²² T. Okusawa,⁴⁰ R. Oldeman,²⁹ R. Orava,²¹ W. Orejudos,²⁸ K. Osterberg,²¹ C. Pagliarone,⁴⁴ E. Palencia,¹⁰ R. Paoletti,⁴⁴ V. Papadimitriou,¹⁵ A. A. Paramonov,¹² S. Pashapour,³² J. Patrick,¹⁵ G. Pauletta,⁵³ M. Paulini,¹¹ C. Paus,³¹ D. Pellett,⁶ A. Penzo,⁵³ T. J. Phillips,¹⁴ G. Piacentino,⁴⁴ J. Piedra,¹⁰ K. T. Pitts,²³ C. Plager,⁷ L. Pondrom,⁵⁸ G. Pope,⁴⁵ X. Portell,³ O. Poukhov,¹³ N. Pounder,⁴¹ F. Prakoshyn,¹³ T. Pratt,²⁹ A. Pronko,¹⁶ J. Proudfoot,² F. Ptohos,¹⁷ G. Punzi,⁴⁴ J. Rademacker,⁴¹ M. A. Rahaman,⁴⁵ A. Rakitine,³¹ S. Rappoccio,²⁰ F. Ratnikov,⁵⁰ H. Ray,³³ B. Reisert,¹⁵ V. Rekovic,³⁶ P. Renton,⁴¹ M. Rescigno,⁴⁹ F. Rimondi,⁴ K. Rinnert,²⁵ L. Ristori,⁴⁴ W. J. Robertson,¹⁴ A. Robson,¹⁹ T. Rodrigo,¹⁰ S. Rolli,⁵⁵ R. Roser,¹⁵ R. Rossin,¹⁶ C. Rott,⁴⁶ J. Russ,¹¹ V. Rusu,¹² A. Ruiz,¹⁰ D. Ryan,⁵⁵ H. Saarikko,²¹ S. Sabik,³² A. Safonov,⁶ R. St. Denis,¹⁹ W. K. Sakumoto,⁴⁷ G. Salamanna,⁴⁹ D. Saltzberg,⁷ C. Sanchez,³ L. Santi,⁵³ S. Sarkar,⁴⁹ K. Sato,⁵⁴ P. Savard,³² A. Savoy-Navarro,¹⁵ P. Schlabach,¹⁵ E. E. Schmidt,¹⁵ M. P. Schmidt,⁵⁹ M. Schmitt,³⁷ T. Schwarz,³³ L. Scodellaro,¹⁰ A. L. Scott,⁹ A. Scribano,⁴⁴ F. Scuri,⁴⁴ A. Sedov,⁴⁶ S. Seidel,³⁶ Y. Seiya,⁴⁰ A. Semenov,¹³ F. Semeria,⁴ L. Sexton-Kennedy,¹⁵ I. Sfiligoi,¹⁷ M. D. Shapiro,²⁸ T. Shears,²⁹ P. F. Shepard,⁴⁵ D. Sherman,²⁰ M. Shimojima,⁵⁴ M. Shochet,¹² Y. Shon,⁵⁸ I. Shreyber,³⁵ A. Sidoti,⁴⁴ A. Sill,⁵² P. Sinervo,³² A. Sisakyan,¹³ J. Sjolin,⁴¹ A. Skiba,²⁵ A. J. Slaughter,¹⁵ K. Sliwa,⁵⁵ D. Smirnov,³⁶ J. R. Smith,⁶ F. D. Snider,¹⁵ R. Snihur,³² M. Soderberg,³³ A. Soha,⁶ S. V. Somalwar,⁵⁰ J. Spalding,¹⁵ M. Spezziga,⁵² F. Spinella,⁴⁴ P. Squillacioti,⁴⁴ H. Stadie,²⁵ M. Stanitzki,⁵⁹ B. Stelzer,³² O. Stelzer-Chilton,³² D. Stentz,³⁷ J. Strologas,³⁶ D. Stuart,⁹ J. S. Suh,²⁷ A. Sukhanov,¹⁶ K. Sumorok,³¹ H. Sun,⁵⁵ T. Suzuki,⁵⁴ A. Taffard,²³ R. Tafifout,³² H. Takano,⁵⁴ R. Takashima,³⁹ Y. Takeuchi,⁵⁴ K. Takikawa,⁵⁴ M. Tanaka,² R. Tanaka,³⁹ N. Tanimoto,³⁹ M. Tecchio,³³ P. K. Teng,¹ K. Terashi,⁴⁸ R. J. Tesarek,¹⁵ S. Tether,³¹ J. Thom,¹⁵ A. S. Thompson,¹⁹ E. Thomson,⁴³ P. Tipton,⁴⁷ V. Tiwari,¹¹ S. Tkaczyk,¹⁵ D. Toback,⁵¹ K. Tollefson,³⁴ T. Tomura,⁵⁴ D. Tonelli,⁴⁴ M. Tönnesmann,³⁴ S. Torre,⁴⁴ D. Torretta,¹⁵ W. Trischuk,³² R. Tsuchiya,⁵⁶ S. Tsuno,³⁹ D. Tsybychev,¹⁶ N. Turini,⁴⁴ J. Tuttle,¹⁴ F. Ukegawa,⁵⁴ T. Unverhau,¹⁹ S. Uozumi,⁵⁴ D. Usynin,⁴³ L. Vacavant,²⁸ A. Vaiciulis,⁴⁷ A. Varganov,³³ S. Vejcik III,¹⁵ G. Velev,¹⁵ V. Vespremi,⁴⁶ G. Veramendi,²³ T. Vickey,²³ R. Vidal,¹⁵ I. Vila,¹⁰ R. Vilar,¹⁰ I. Vollrath,³² I. Volobouev,²⁸ M. von der Mey,⁷ P. Wagner,⁵¹ R. G. Wagner,² R. L. Wagner,¹⁵ W. Wagner,²⁵ R. Wallny,⁷ T. Walter,²⁵ Z. Wan,⁵⁰ M. J. Wang,¹ S. M. Wang,¹⁶ A. Warburton,³² B. Ward,¹⁹ S. Waschke,¹⁹ D. Waters,³⁰ T. Watts,⁵⁰ M. Weber,²⁸ W. C. Wester III,¹⁵ B. Whitehouse,⁵⁵ D. Whiteson,⁴³ A. B. Wicklund,² E. Wicklund,¹⁵ H. H. Williams,⁴³ P. Wilson,¹⁵ B. L. Winer,³⁸ P. Wittich,⁴³ S. Wolbers,¹⁵ C. Wolfe,¹² M. Wolter,⁵⁵ M. Worcester,⁷ S. Worm,⁵⁰ T. Wright,³³ X. Wu,¹⁸ F. Würthwein,⁸ A. Wyatt,³⁰ A. Yagil,¹⁵ T. Yamashita,³⁹ K. Yamamoto,⁴⁰ J. Yamaoka,⁵⁰ C. Yang,⁵⁹ U. K. Yang,¹² W. Yao,²⁸ G. P. Yeh,¹⁵ J. Yoh,¹⁵ K. Yorita,⁵⁶ T. Yoshida,⁴⁰ I. Yu,²⁷ S. Yu,⁴³ J. C. Yun,¹⁵ L. Zanello,⁴⁹ A. Zanetti,⁵³ I. Zaw,²⁰ F. Zetti,⁴⁴ J. Zhou,⁵⁰ and S. Zucchelli⁴

(CDF Collaboration)

¹*Institute of Physics, Academia Sinica, Taipei, Taiwan 11529, Republic of China*²*Argonne National Laboratory, Argonne, Illinois 60439, USA*³*Institut de Fisica d'Altes Energies, Universitat Autònoma de Barcelona, E-08193, Bellaterra (Barcelona), Spain*⁴*Istituto Nazionale di Fisica Nucleare, University of Bologna, I-40127 Bologna, Italy*⁵*Brandeis University, Waltham, Massachusetts 02254, USA*⁶*University of California, Davis, Davis, California 95616, USA*⁷*University of California, Los Angeles, Los Angeles, California 90024, USA*⁸*University of California, San Diego, La Jolla, California 92093, USA*⁹*University of California, Santa Barbara, Santa Barbara, California 93106, USA*¹⁰*Instituto de Fisica de Cantabria, CSIC-University of Cantabria, 39005 Santander, Spain*¹¹*Carnegie Mellon University, Pittsburgh, Pennsylvania 15213, USA*¹²*Enrico Fermi Institute, University of Chicago, Chicago, Illinois 60637, USA*¹³*Joint Institute for Nuclear Research, RU-141980 Dubna, Russia*¹⁴*Duke University, Durham, North Carolina 27708, USA*¹⁵*Fermi National Accelerator Laboratory, Batavia, Illinois 60510, USA*¹⁶*University of Florida, Gainesville, Florida 32611, USA*¹⁷*Laboratori Nazionali di Frascati, Istituto Nazionale di Fisica Nucleare, I-00044 Frascati, Italy*¹⁸*University of Geneva, CH-1211 Geneva 4, Switzerland*¹⁹*Glasgow University, Glasgow G12 8QQ, United Kingdom*²⁰*Harvard University, Cambridge, Massachusetts 02138, USA*²¹*Division of High Energy Physics, Department of Physics, University of Helsinki**and Helsinki Institute of Physics, FIN-00044, Helsinki, Finland*²²*Hiroshima University, Higashi-Hiroshima 724, Japan*²³*University of Illinois, Urbana Illinois 61801, USA*

²⁴*The Johns Hopkins University, Baltimore, Maryland 21218, USA*²⁵*Institut für Experimentelle Kernphysik, Universität Karlsruhe, 76128 Karlsruhe, Germany*²⁶*High Energy Accelerator Research Organization (KEK), Tsukuba, Ibaraki 305, Japan*²⁷*Center for High Energy Physics: Kyungpook National University, Taegu 702-701; Seoul National University, Seoul 151-742; and SungKyunKwan University, Suwon 440-746; Korea*²⁸*Ernest Orlando Lawrence Berkeley National Laboratory, Berkeley, California 94720, USA*²⁹*University of Liverpool, Liverpool L69 7ZE, United Kingdom*³⁰*University College London, London WC1E 6BT, United Kingdom*³¹*Massachusetts Institute of Technology, Cambridge, Massachusetts 02139, USA*³²*Institute of Particle Physics: McGill University, Montréal, Canada H3A 2T8 and University of Toronto, Toronto, Canada M5S 1A7*³³*University of Michigan, Ann Arbor, Michigan 48109, USA*³⁴*Michigan State University, East Lansing, Michigan 48824, USA*³⁵*Institution for Theoretical and Experimental Physics, ITEP, Moscow 117259, Russia*³⁶*University of New Mexico, Albuquerque, New Mexico 87131, USA*³⁷*Northwestern University, Evanston, Illinois 60208, USA*³⁸*The Ohio State University, Columbus, Ohio 43210, USA*³⁹*Okayama University, Okayama 700-8530, Japan*⁴⁰*Osaka City University, Osaka 588, Japan*⁴¹*University of Oxford, Oxford OX1 3RH, United Kingdom*⁴²*University of Padova, Istituto Nazionale di Fisica Nucleare, Sezione di Padova-Trento, I-35131 Padova, Italy*⁴³*University of Pennsylvania, Philadelphia, Pennsylvania 19104, USA*⁴⁴*Istituto Nazionale di Fisica Nucleare Pisa, Universities of Pisa, Siena and Scuola Normale Superiore, I-56127, Italy*⁴⁵*University of Pittsburgh, Pittsburgh, Pennsylvania 15260, USA*⁴⁶*Purdue University, West Lafayette, Indiana 47907, USA*⁴⁷*University of Rochester, Rochester, New York 14627, USA*⁴⁸*The Rockefeller University, New York, New York 10021, USA*⁴⁹*Istituto Nazionale di Fisica Nucleare, Sezione di Roma 1, University di Roma “La Sapienza”, I-00185 Roma, Italy*⁵⁰*Rutgers University, Piscataway, New Jersey 08855, USA*⁵¹*Texas A & M University, College Station, Texas 77843, USA*⁵²*Texas Tech University, Lubbock, Texas 79409, USA*⁵³*Istituto Nazionale di Fisica Nucleare, University of Trieste/Udine, Italy*⁵⁴*University of Tsukuba, Tsukuba, Ibaraki 305, Japan*⁵⁵*Tufts University, Medford, Massachusetts 02155, USA*⁵⁶*Waseda University, Tokyo 169, Japan*⁵⁷*Wayne State University, Detroit, Michigan 48201, USA*⁵⁸*University of Wisconsin, Madison, Wisconsin 53706, USA*⁵⁹*Yale University, New Haven, Connecticut 06520, USA*

(Received 3 March 2005; published 11 August 2005)

We present a search for long-lived doubly charged Higgs bosons ($H^{\pm\pm}$), with signatures of high ionization energy loss and muonlike penetration. We use 292 pb^{-1} of data collected in $p\bar{p}$ collisions at $\sqrt{s} = 1.96 \text{ TeV}$ by the CDF II detector at the Fermilab Tevatron. Observing no evidence of long-lived doubly charged particle production, we exclude $H_L^{\pm\pm}$ and $H_R^{\pm\pm}$ bosons with masses below $133 \text{ GeV}/c^2$ and $109 \text{ GeV}/c^2$, respectively. In the degenerate case we exclude $H^{\pm\pm}$ mass below $146 \text{ GeV}/c^2$. All limits are quoted at the 95% confidence level.

DOI: 10.1103/PhysRevLett.95.071801

PACS numbers: 14.80.Cp, 12.60.Fr, 13.85.Rm

The electroweak gauge symmetry of the standard model (SM) is broken by the hypothetical Higgs mechanism, thereby imparting masses to the W and Z bosons, the mediators of the weak force. A number of models [1–4] extend the SM Higgs sector to include additional symmetries. For instance, the left-right symmetric model [2] postulates a right-handed version of the weak interaction, whose gauge symmetry is spontaneously broken at a high mass scale, leading to the parity-violating SM. This model is supported by recent data on neutrino oscillations [5], and explains small neutrino masses [6]. The model generally requires a Higgs triplet containing a doubly charged Higgs

boson ($H^{\pm\pm}$), which could be light in the minimal supersymmetric left-right model [3,4]. Discovery of the $H^{\pm\pm}$ boson would not only shed light on the Higgs mechanism, but also provide evidence for new symmetries beyond the SM. Grand unified theories containing Higgs triplets and their relevance for neutrino masses and mixing are reviewed in [7], while “Little Higgs” models that ameliorate the hierarchy and fine-tuning problems of the SM are reviewed in [8].

The dominant production mode at the Tevatron is $p\bar{p} \rightarrow \gamma^*/Z + X \rightarrow H^{++}H^{--} + X$, whose cross section at tree level is specified by the quantum numbers and the mass

$(m_{H^{\pm\pm}})$ of the $H^{\pm\pm}$ boson. The partial width in the leptonic decay modes is given by $\Gamma_{ll'} = h_{ll'}^2 m_{H^{\pm\pm}}/(8\pi)$, where $h_{ll'}$ are phenomenological couplings. In a previous Letter [9], we published the most stringent $H^{\pm\pm}$ mass limits from direct searches in the ee , $e\mu$, and $\mu\mu$ decay channels for $0.5 > h_{ll'} > 10^{-5}$. In this Letter, we discuss the case where the $H^{\pm\pm}$ boson lifetime (τ) is long ($c\tau > 3$ m, corresponding to $h_{ll'} < 10^{-8}$), resulting in the $H^{\pm\pm}$ boson decaying outside the CDF detector [10]. A supersymmetric left-right model [4] has predicted a light $H^{\pm\pm}$ boson with $B - L = 0$, where B and L represent baryon number and lepton number, respectively, resulting in $h_{ll'} = 0$ and a long lifetime [9]. The LEP experiments have set limits on a long-lived $H^{\pm\pm}$ boson [11,12], with the best limit coming from the DELPHI experiment [12], excluding $m_{H^{\pm\pm}} < 99.6 \text{ GeV}/c^2$ ($99.3 \text{ GeV}/c^2$) at the 95% confidence level (C.L.) for $H^{\pm\pm}$ bosons with couplings to left- (right-) handed leptons. Our search for pair production of long-lived, doubly charged particles is based on the signatures of increased ionization energy loss and muonlike penetration of shielding (due to their large mass). We set the most stringent $H^{\pm\pm}$ mass limits in the context of the left-right symmetric model.

This analysis uses $292 \pm 18 \text{ pb}^{-1}$ of data collected by the CDF II detector [13] in $p\bar{p}$ collisions at $\sqrt{s} = 1.96 \text{ TeV}$ at the Tevatron. The detector consists of a cylindrical magnetic spectrometer with silicon and drift chamber trackers, surrounded by a time-of-flight system, preshower detectors, electromagnetic (EM) and hadronic calorimeters, and muon detectors. The central drift chamber [central outer tracker (COT)] [14], central calorimeter [15], and the muon detectors [16] covering the region $|\eta| < 1$ [17] are used in this analysis. The COT and calorimeter provide ionization information in addition to tracking and identification of penetrating particles.

We use an inclusive muon trigger requiring a COT track with transverse momentum $p_T > 18 \text{ GeV}/c$ [17], and a matching track segment in the central muon chambers. In the offline analysis, we search for $H^{++}H^{--}$ pair production by requiring two COT tracks, each with $p_T > 20 \text{ GeV}/c$, beam impact parameter $< 2 \text{ mm}$, and at least 30 (out of a maximum of 96) sense wire hits. At least one of the tracks is required to have a matching muon chamber segment. We also require their isolation $I_{0.4} < 0.1$, where $I_{0.4}$ is the ratio of the total calorimeter E_T [17] around the track within a cone of angle $R \equiv \sqrt{(\Delta\eta)^2 + (\Delta\phi)^2} = 0.4$ to the track p_T [17]. Energy deposited by the particle is excluded from the calculation of $I_{0.4}$. Finally, we tag and reject cosmic-ray tracks using an algorithm based on COT hit timing [18], whose efficiency is measured to be $100^{+0.0}_{-0.8}\%$ for collider muons and leaves negligible cosmic-ray contamination.

We use $Z \rightarrow \mu\mu$ events that were triggered by one of the muons to measure trigger and offline identification efficiencies of the other muon. The track selection efficiency is

$(93.6 \pm 0.2)\%$, and the efficiency for one of the two $H^{\pm\pm}$ bosons to satisfy the muon trigger and matching-segment requirements is $(96.8 \pm 0.7)\%$. The effect of increased multiple-scattering of doubly charged particles is investigated by comparing the segment matching efficiency for muons from Z boson decays with that for lower- p_T muons from Y decays. The small ($\approx 0.5\%$) difference, when scaled as p_T^{-1} to the large p_T of $H^{\pm\pm}$ tracks, predicts a negligible ($\approx 0.2\%$) correction. About 3% of $H^{\pm\pm}$ particles are expected to be sufficiently slow ($\beta < 0.4$) to have a reduced efficiency due to delayed hits, for a net efficiency loss of 0.4%. A correction is applied to the track selection efficiency for $H^{\pm\pm}$ bosons passing near a calorimeter tower edge and depositing a large ionization energy signal in an adjacent tower. This effect, caused by the resolution of the track extrapolation, leads to the $H^{\pm\pm}$ boson candidate failing the isolation requirement. This geometrical correction results in an overall $H^{\pm\pm}$ track selection efficiency of $(89 \pm 4)\%$.

The charge collected by each COT wire is proportional to the ionization deposited by the particle per unit length (dE/dx), and is encoded in the width of the digital pulse generated by the front-end electronics [14]. Off-line corrections are applied for the electronics response, track polar angle, COT high voltage, drift distance, drift direction with respect to track direction, gas pressure, attenuation along the sense wire, radial location of the sense wire, and time. The mean number of hits on our selected tracks is 85. The mean (w) of the lower 80% of the corrected widths of all recorded hits of a track is used as a measure of its ionization energy loss. The use of the truncated mean reduces the sensitivity to Landau fluctuations.

The most probable dE/dx for a minimum-ionizing particle corresponds to $w \approx 15 \text{ ns}$, as seen from the cosmic-ray muon distribution in Fig. 1. For the $H^{\pm\pm}$ search we require $w > 35 \text{ ns}$. The w distribution of the latter is modeled by quadrupling the w measurements of cosmic-

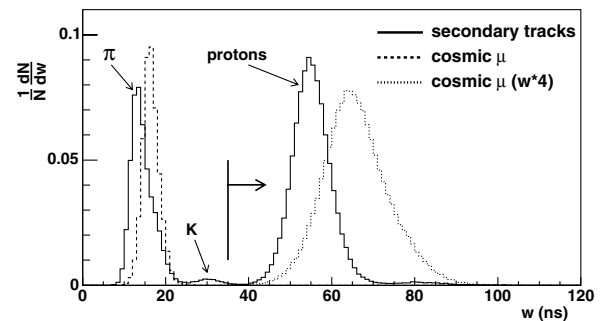


FIG. 1. The distribution of the COT dE/dx variable w for positively charged secondary [19] tracks in the momentum range of $300\text{--}350 \text{ MeV}/c$ (solid line), for high- p_T cosmic-ray muons (dashed line), and the expectation for $H^{\pm\pm}$ tracks (dotted line). The latter is modeled by quadrupling the w measurements of cosmic-ray muons. The arrow indicates the signal selection region.

ray muons, as given by the (charge)² dependence of ionization energy loss in the Bethe-Bloch equation. We use low-momentum protons from secondary interactions to measure the efficiency of the dE/dx cut on $H^{\pm\pm}$ tracks, which are expected to have similar or greater dE/dx than said protons (see Fig. 1). We obtain a control sample enriched in highly ionizing protons by selecting low-momentum positively charged secondary [19] tracks. The pion contribution is statistically removed by subtracting the w distribution of negatively charged secondary tracks. Using the resulting w distribution of protons, we measure the w selection efficiency to be $>99.5\%$.

We perform two simultaneous searches with “loose” and “tight” selections for highly ionizing particles. The loose selection, based on the COT dE/dx measurement only, yields the maximum acceptance, while the tight selection also requires large EM and hadronic calorimeter signals for confirmation of a potential signal. We make the *a priori* decision to use the results from the loose search to quote an upper limit on the signal cross section and the tight search results to quote a statistically significant observation of signal. The most probable ionization energy signal deposited by muons in the EM and hadronic calorimeters (referred to as E_{EM} and E_{had} , respectively) is 0.3 GeV and 1.7 GeV, respectively, for normal incidence. For the tight $H^{\pm\pm}$ search we require $E_{EM} > 0.6$ GeV and $E_{had} > 4$ GeV. The efficiency of the calorimeter ionization requirements is $(81.1 \pm 0.1)\%$, measured by quadrupling E_{EM} and E_{had} of a pure cosmic-ray sample to model the $H^{\pm\pm}$ energy deposition.

We calculate the geometric and kinematic acceptance for a pair of $H^{\pm\pm}$ bosons using the PYTHIA [20] generator and a GEANT [21]-based detector simulation. The acceptance increases from 38.4% at $m_{H^{\pm\pm}} = 90$ GeV/c² to 46.8% at $m_{H^{\pm\pm}} = 160$ GeV/c², with the dominant relative systematic uncertainty of 1% due to parton distribution functions (PDFs) [22]. Systematic uncertainties due to momentum scale and resolution are negligible. The geometric and kinematic acceptance is multiplied by the loose event selection efficiency of $(72.9 \pm 6.6)\%$ to obtain the overall signal acceptance for the loose search.

Backgrounds arise from (1) jets fragmenting into high- p_T tracks, (2) $Z \rightarrow ee$, (3) $Z \rightarrow \mu\mu$, and

TABLE I. Summary of fake rate measurements. The e , μ , and τ fake rates and the “muon fake rates” for jets are quoted as upper limits at the 68% C.L., since no events in the respective control samples pass the $H^{\pm\pm}$ selection cuts.

Source	Loose search		Tight Search	
	“Track”	“Muon”	Track	Muon
jet ($\times 10^{-4}$)	$3.2^{+5.0}_{-2.9}$	<0.05	$0.28^{+0.04}_{-0.05}$	<0.05
$e(\times 10^{-6})$	<4	<0.00009	<0.05	<0.00002
$\mu(\times 10^{-6})$	<7	<7	<0.02	<0.02
$\tau(\times 10^{-5})$	<2	<0.002	<2	<0.002

(4) $Z \rightarrow \tau\tau$ where at least one τ decays hadronically. The backgrounds are a result of muon misidentification and dE/dx mismeasurement, which can arise from overlapping particles. Each background is estimated by multiplying the number of misidentifiable events by the product of the appropriate misidentification probabilities (fake rates). Fake rates are measured with and without the requirement of a matching muon chamber segment. We refer to these as the “muon fake rate” and “track fake rate,” respectively. A fake rate is defined as the probability that a track (or muon) passing certain loose identification cuts also satisfies the analysis cuts. For jets, electrons, and τ 's, the muon fake rate is obtained by multiplying the track fake rate by the estimated probability of mismatching a muon chamber segment to the track.

The track fake rate and muon fake rate for jets are measured from jet-triggered data and muon-triggered data, respectively. The variation of the fake rates with p_T and jet proximity is taken as a measure of systematic uncertainty. The number of misidentifiable jet events is given by the number of muon-triggered data events containing a loosely selected muon and another loosely selected track. Fake rates for electrons and hadronically decaying τ 's are estimated from the GEANT-based detector simulation. These fake rate measurements are limited by Monte Carlo statistics, as no Monte Carlo events pass the $H^{\pm\pm}$ selection cuts. The number of misidentifiable $Z \rightarrow ee$ events is obtained from the $Z \rightarrow ee$ data sample, corrected for electron efficiencies and normalized to the luminosity of the muon-triggered signal sample. The number of $Z \rightarrow \tau\tau$ misidentifiable events is obtained from the number of $Z \rightarrow \mu\mu$ events observed in the data, assuming $\mu\tau$ universality, and correcting for muon efficiencies. Finally, fake rates for muons are measured from a pure sample of cosmic rays, which are again statistically limited as no events pass the $H^{\pm\pm}$ selection cuts. The number of misidentifiable events is given by the number of $Z \rightarrow \mu\mu$ data events selected with the loose cuts. Table I summarizes the fake rate measurements, and Table II summarizes the resulting background estimates.

No $H^{++}H^{--}$ candidate events are found in the data. The null result is used to set upper limits on the number of signal events (3.2 at the 95% C.L.) and the $H^{\pm\pm}$ pair-production cross section using a Bayesian [23] approach,

TABLE II. Summary of the estimated number of background events (quoted as 68% C.L. upper limits) and the observed number of events in the data.

Background	Loose Search	Tight Search
Jet	$<3 \times 10^{-5}$	$<3 \times 10^{-6}$
$Z \rightarrow ee$	$<1 \times 10^{-11}$	$<2 \times 10^{-14}$
$Z \rightarrow \mu\mu$	$<4 \times 10^{-7}$	$<4 \times 10^{-12}$
$Z \rightarrow \tau\tau$	$<8 \times 10^{-9}$	$<8 \times 10^{-9}$
Data	0	0

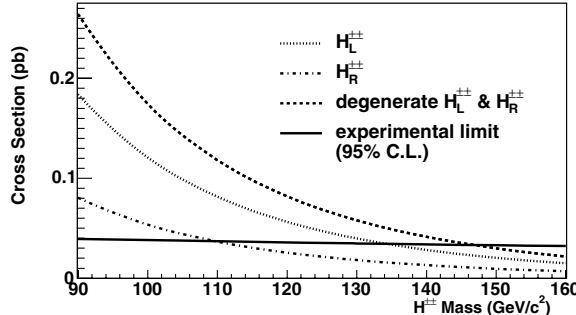


FIG. 2. The comparison of the experimental cross section upper limit with the theoretical next-to-leading order cross section [25] for pair production of $H^{\pm\pm}$ bosons. The theoretical cross sections are computed separately for bosons with left-handed ($H_L^{\pm\pm}$) and right-handed ($H_R^{\pm\pm}$) couplings, and summed for the case that their masses are degenerate.

with a flat prior for the signal cross section and Gaussian priors for the uncertainties on acceptance, background, and integrated luminosity (6%) [24]. The 95% C.L. upper limit on the cross section (which varies from 39.7 fb at $m_{H^{\pm\pm}} = 90$ GeV/ c^2 to 32.6 fb at $m_{H^{\pm\pm}} = 160$ GeV/ c^2 , see Fig. 2) is converted into an $H^{\pm\pm}$ mass limit by comparing to the theoretical $p\bar{p} \rightarrow \gamma^*/Z + X \rightarrow H^{++}H^{--} + X$ cross section at next-to-leading order [25] using the CTEQ6 [22] set of PDFs. We include uncertainties in the theoretical cross sections due to PDFs (5%) [22] and higher-order QCD corrections (7.5%) [25] in the extraction of the mass limit, for a total systematic uncertainty of 14%. The theoretical cross sections are computed separately for $H_L^{\pm\pm}$ and $H_R^{\pm\pm}$ bosons that couple to left- and right-handed particles, respectively. When only one of these states is accessible, we exclude the long-lived $H_L^{\pm\pm}$ boson below a mass of 133 GeV/ c^2 and the long-lived $H_R^{\pm\pm}$ boson below a mass of 109 GeV/ c^2 , both at the 95% C.L. When the two states are degenerate in mass, we exclude $m_{H^{\pm\pm}} < 146$ GeV/ c^2 at the 95% C.L.

In conclusion, we have searched for long-lived doubly charged particles using their signatures of high ionization and muonlike penetration. No evidence is found for pair-production of such particles, and we set the individual lower limits of 133 GeV/ c^2 and 109 GeV/ c^2 , respectively, on the masses of long-lived $H_L^{\pm\pm}$ and $H_R^{\pm\pm}$ bosons. The mass limit for the case of degenerate $H_L^{\pm\pm}$ and $H_R^{\pm\pm}$ bosons is 146 GeV/ c^2 .

We thank M. Mühlleitner and M. Spira for calculating the next-to-leading order $H^{\pm\pm}$ production cross section. We thank the Fermilab staff and the technical staffs of the participating institutions for their vital contributions. This work was supported by the U.S. Department of Energy and National Science Foundation; the Italian Istituto Nazionale di Fisica Nucleare; the Ministry of Education, Culture, Sports, Science, and Technology of Japan; the Natural Sciences and Engineering Research Council of Canada; the National Science Council of the Republic of China; the

Swiss National Science Foundation; the A.P. Sloan Foundation; the Bundesministerium fuer Bildung und Forschung, Germany; the Korean Science and Engineering Foundation and the Korean Research Foundation; the Particle Physics and Astronomy Research Council and the Royal Society, UK; the Russian Foundation for Basic Research; the Commission Interministerial de Ciencia y Tecnologia, Spain; and in part by the European Community's Human Potential Programme under Contract No. HPRN-CT-2002-00292, Probe for New Physics.

- [1] T. P. Cheng and L.-F. Li, Phys. Rev. D **22**, 2860 (1980).
- [2] R. N. Mohapatra and J.C. Pati, Phys. Rev. D **11**, 566 (1975); G. Senjanovic and R.N. Mohapatra, Phys. Rev. D **12**, 1502 (1975); R.N. Mohapatra and G. Senjanovic, Phys. Rev. D **23**, 165 (1981).
- [3] C. S. Aulakh, A. Melfo, and G. Senjanovic, Phys. Rev. D **57**, 4174 (1998); Z. Chacko and R.N. Mohapatra, Phys. Rev. D **58**, 015003 (1998).
- [4] C. S. Aulakh, K. Benakli, and G. Senjanovic, Phys. Rev. Lett. **79**, 2188 (1997).
- [5] Y. Ashie *et al.* (Super-Kamiokande Collaboration), Phys. Rev. Lett. **93**, 101801 (2004), and references therein.
- [6] R. N. Mohapatra and G. Senjanovic, Phys. Rev. Lett. **44**, 912 (1980).
- [7] B. Bajc, G. Senjanovic, and F. Vissani, Phys. Rev. D **70**, 093002 (2004), and references therein; S. F. King, Rep. Prog. Phys. **67**, 107 (2004), and references therein.
- [8] T. Han, H. E. Logan, B. McElrath, and L.-T. Wang, Phys. Rev. D **67**, 095004 (2003).
- [9] D. Acosta *et al.* (CDF Collaboration), Phys. Rev. Lett. **93**, 221802 (2004).
- [10] The range $10^{-5} > h_{H'} > 10^{-8}$ corresponds to the $H^{\pm\pm}$ boson decaying within the detector, and requires other triggering and tracking methods.
- [11] G. Abbiendi *et al.* (OPAL Collaboration), Phys. Lett. B **526**, 221 (2002).
- [12] J. Abdallah *et al.* (DELPHI Collaboration), Phys. Lett. B **552**, 127 (2003).
- [13] D. Acosta *et al.*, Phys. Rev. D **71**, 032001 (2005).
- [14] T. Affolder *et al.*, Nucl. Instrum. Methods Phys. Res., Sect. A **526**, 249 (2004).
- [15] F. Abe *et al.* (CDF Collaboration), Nucl. Instrum. Methods Phys. Res., Sect. A **271**, 387 (1988).
- [16] G. Ascoli *et al.*, Nucl. Instrum. Methods Phys. Res., Sect. A **268**, 33 (1988).
- [17] CDF uses a cylindrical coordinate system in which ϕ is the azimuthal angle, r is the radius from the nominal beamline, and $+z$ points in the direction of the proton beam and is zero at the center of the detector. The pseudorapidity $\eta = -\ln[\tan(\theta/2)]$, where θ is the polar angle with respect to the z axis. Calorimeter energy (track momentum) measured transverse to the beam is denoted as $E_T(p_T)$. Track p_T is evaluated from its curvature assuming a singly charged particle, and is half of the true p_T for a doubly charged particle.

- [18] A. V. Kotwal, H. K. Gerberich, and C. Hays, Nucl. Instrum. Methods Phys. Res., Sect. A **506**, 110 (2003).
- [19] “Secondary” tracks are those produced in secondary interactions with detector material, and are selected by requiring beam impact parameter >1 cm.
- [20] T. Sjöstrand, Comput. Phys. Commun. **82**, 74 (1994).
- [21] R. Brun and F. Carminati, CERN Program Library Long Writeup, No. W5013, 1993 (unpublished), version 3.15.
- [22] J. Pumplin *et al.*, J. High Energy Phys. 07 (2002) 012.
- [23] K. Hagiwara *et al.* (Particle Data Group), Phys. Rev. D **66**, 010001 (2002); I. Bertram *et al.*, Fermilab Report No. Fermilab-TM-2104, 2000 (unpublished). The numerical error caused by the upper cutoff in the numerical integration of the posterior likelihood is 0.005%.
- [24] S. Klimenko, J. Konigsberg, and T. M. Liss, Fermilab Report No. Fermilab-FN-0741, 2003 (unpublished).
- [25] M. Mühlleitner and M. Spira, Phys. Rev. D **68**, 117701 (2003). The cross sections have theoretical uncertainties of 5%–10% due to QCD corrections.